JACC: CLINICAL ELECTROPHYSIOLOGY
VOL. 1, NO. 5, 2015

ISSN 2405-500X/$36.00
PUBLISHED BY ELSEVIER INC.
http://dx.doi.org/10.1016/j.jacep.2015.07.006

NEW RESEARCH PAPERS

Scar Extension Measured by Magnetic Resonance–Based Signal Intensity Mapping Predicts Ventricular Tachycardia Recurrence After Substrate Ablation in Patients With Previous Myocardial Infarction

Pablo Ávila, MD,* Esther Pérez-David, MD, PhD,* Maite Izquierdo, MD, PhD,† Antonio Rojas-González, MD,* Juan M. Sánchez-Gómez, MD,† María J. Ledesma-Carbayo, PhD,‡ M. Pilar López-Lereu, MD, PhD,§ Gerard Loughlin, MD,* José V. Monmeneu, MD, PhD,§ Esteban González-Torrecilla, MD, PhD,* Felipe Atienza, MD, PhD,* Tomas Datino, MD, PhD,* Loreto Bravo, MD,* Javier Bermejo, MD, PhD,* Francisco Fernández-Avilés, MD, PhD,* Ricardo Ruíz-Granel, MD, PhD,† Ángel Arenal, MD, PhD*

ABSTRACT

OBJECTIVES The aim of this study was to determine if noninvasive measurement of scar by contrast-enhanced magnetic resonance imaging (MRI)–based signal intensity (SI) mapping predicts ventricular tachycardia (VT) recurrence after endocardial ablation.

BACKGROUND Scar extension on voltage mapping predicts VT recurrence after ablation procedures.

METHODS A total of 46 consecutive patients with previous myocardial infarction (87% men, mean age 68 ± 9 years, mean left ventricular ejection fraction 36 ± 10%) who underwent VT substrate ablation before the implantation of a cardioverter-defibrillator were included. Before ablation, contrast-enhanced MRI was performed, and areas of endocardial and epicardial scarring and heterogeneous tissue were measured; averaged subendocardial and subepicardial signal intensities were projected onto 3-dimensional endocardial and epicardial shells in which dense scar, heterogeneous tissue, and normal tissue were differentiated.

RESULTS During a mean follow-up period of 32 ± 24 months 17 patients (37%) had VT recurrence. Patients with recurrence had larger scar and heterogeneous tissue areas on SI maps in both endocardium (81 ± 27 cm^2 vs. 48 ± 21 cm^2 [p = 0.001] and 53 ± 21 cm^2 vs. 30 ± 15 cm^2 [p = 0.001], respectively) and epicardium (76 ± 28 cm^2 vs. 51 ± 29 cm^2 [p = 0.032] and 59 ± 25 cm^2 vs. 37 ± 19 cm^2 [p = 0.008]). In the multivariate analysis, MRI endocardial scar extension was the only independent predictor of VT recurrence (hazard ratio: 1.310 [per 10 cm^2]; 95% confidence interval: 1.051 to 1.632; p = 0.034). Freedom from VT recurrence was higher in patients with small endocardial scars by MRI (<65 cm^2) than in those with larger scars (≥65 cm^2) (85% vs. 20%, log-rank p = 0.018).

CONCLUSIONS Pre-procedure endocardial scar extension assessment by contrast-enhanced MRI predicts VT recurrence after endocardial substrate ablation. This information may be useful to select patients for ablation procedures.
(J Am Coll Cardiol EP 2015;1:353–65) © 2015 by the American College of Cardiology Foundation.

Listen to this manuscript's audio summary by *JACC: Clinical Electrophysiology* Editor-in-Chief Dr. David J. Wilber.

From the *Department of Cardiology, Instituto de Investigación Sanitaria, Hospital General Universitario Gregorio Marañón, Universidad Complutense, Madrid, Spain; †Department of Cardiology, Hospital Clínico Universitario, Valencia, Spain; ‡Universidad Politécnica de Madrid and CIBER-BBN, Madrid, Spain; and the §Cardiac Imaging Unit, ERESA, Valencia, Spain.

JACC: CLINICAL ELECTROPHYSIOLOGY VOL. 1, NO. 5, 2015
OCTOBER 2015:353–65

ABBREVIATIONS AND ACRONYMS

CC = conduction channel

CI = confidence interval

ECG = electrocardiogram

EIC-LP = electrogram with isolated components and/or late potentials

HT = heterogeneous tissue

ICD = implantable cardioverter-defibrillator

IQR = interquartile range

LVEF = left ventricular ejection fraction

MRI = magnetic resonance imaging

RF = radiofrequency

SI = signal intensity

SMVT = sustained monomorphic ventricular tachycardia

3D = 3-dimensional

VT = ventricular tachycardia

Ventricular tachycardia (VT) ablation reduces arrhythmia recurrence in patients with multiple episodes, and it has been proposed as a therapy in patients receiving implantable cardioverter-defibrillators (ICDs) (1,2). However, this procedure is complex, costly, and not free of serious complications. Identification of ablation responders could optimize the use of this therapy and even permit its use as an alternative to ICD placement in selected patients. Recently, 2 independent studies have shown with similar figures that endocardial scar extension measured on voltage maps predicts VT recurrence after ablation (3,4). These findings may be related to the fact that in patients with large scars, either the complete VT substrate ablation is more difficult to achieve or epicardial VT substrate is more likely (5,6).

SEE PAGE 366

Contrast-enhanced magnetic resonance imaging (MRI) is an accurate technique to identify scar and differentiate dense scar from heterogeneous tissue (HT) (7,8). Both scar and HT extension, analyzed by contrast-enhanced MRI, have proved more valuable for arrhythmogenic risk stratification than left ventricular ejection fraction (LVEF) (9–11). Left ventricular signal intensity (SI) mapping, in which subendocardial and subepicardial SI is averaged and projected onto 3-dimensional (3D) reconstructions of the endocardial and epicardial surfaces, has good correlation with electroanatomic mapping and allows measurement of the extension of endocardial and epicardial HT and scar (12–14).

We hypothesized that the extent of endocardial scar and the presence of epicardial involvement, as assessed by contrast-enhanced MRI-based SI mapping, could determine the risk for VT recurrence after substrate ablation.

METHODS

PATIENT SAMPLE. A total of 46 consecutive patients with chronic myocardial infarction referred for VT ablation to 1 of the 2 participating centers (Hospital Gregorio Marañón, Madrid, Spain, and Hospital Clínico, Valencia, Spain), who had contrast-enhanced MRI performed just before ablation, were included in this study. None of these patients had contraindications to MRI, including ICDs. Those with previous ablation procedures were excluded. After providing informed consent, all patients underwent clinical evaluation and contrast-enhanced MRI, followed by an electrophysiological study. After VT ablation, implantation of ICDs was indicated in all but 4 patients with significant comorbidities. This study complied with the Declaration of Helsinki, and the local ethics committee approved the research protocol.

MRI. All patients underwent contrast-enhanced MRI with a 1.5-T scanner (Intera, Philips Medical Systems, Best, the Netherlands). All images were obtained with electrocardiographic gating and breath-holding. The MRI study consisted of cine steady-state free precession imaging of left ventricular function and late enhancement imaging of myocardial scar tissue. Late enhancement images were obtained 10 to 15 min after an injection of 0.2 mmol/kg of gadodiamide (Omniscan, GE Healthcare, Oslo, Norway). Late-enhanced images were used for infarct characterization. Infarct and HT (i.e., gray zone) mass was quantified by 2 previously described methods: 1) the full width at half maximum (11,15); and 2) on the basis of SDs of the SI from the remote mean healthy myocardium (>2 SDs defined the total infarct mass, >3 SDs the core infarct, and HT between 2 and 3 SDs) (10,16).

Magnetic resonance–based endo-epicardial SI mapping. The myocardial wall was divided into 2 equal parts: subendocardium and subepicardium. The averaged SI of each part was projected respectively onto 3D endocardial and epicardial shell reconstructions of the left ventricle to identify the endocardial and epicardial VT substrate. To achieve this, the left ventricular endocardial and epicardial contours were manually defined on contiguous short-axis slices using QMass MR 7.0 (Medis Medical Imaging, Leiden, the Netherlands) and imported into our tool. Three-dimensional endocardial and epicardial reconstructions were computed off-line from a short-axis contrast-enhanced MRI image volume

This study was partially supported by the National Fund for Health Research (Fondo de Investigación Sanitaria) through grants PI10/02771, TIN2007-68048-C02-01, TIN2007-68048-C02-02, and TEC2010-21619-C04-03 from the Spanish Ministry of Science and Innovation and the Cooperative Cardiovascular Disease Research Network (RD12/0042), Instituto de Salud Carlos III, Ministry of Economy and Competitiveness, Spain. Dr. Arenal is a consultant for Medtronic and Boston Scientific, Spain. Dr. Atienza is a consultant for Medtronic, Spain. All other authors have reported that they have no relationships relevant to the contents of this paper to disclose.

Manuscript received February 17, 2015; revised manuscript received July 20, 2015, accepted July 30, 2015.

using custom software developed in the MATLAB environment (The MathWorks, Natick, Massachusetts). The 3D visualization interface was implemented in Java (Sun Microsystems, Santa Clara, California) using VTK (Kitware, Clifton Park, New York) visualization algorithms (12). The 2 surface maps and short-axis slices were analyzed to determine the structure of the scar and HT in the ventricular wall (endo-epicardial SI mapping). These surfaces were color-coded to provide information on SI: the red area represented dense scar and was defined by an SI greater than or equal to the minimal SI in the core of the scar, the magenta area represented normal myocardium (SI less than or equal to SI peak in the normal myocardium), and the area between these extremes represented HT. On all mapping surfaces, the extension of scar, dense scar, and HT was measured using custom-developed software. We also measured the number of HT channels, which were defined as corridors of HT differentiated from the surrounding scar tissue by lower SI (12). SI processing and measurements were performed in a core laboratory at Gregorio Marañón Hospital, blinded to follow-up data.

ELECTROPHYSIOLOGICAL STUDY. The electrophysiological study was performed 2 to 7 days after contrast-enhanced MRI. At least 2 quadrupolar catheters were placed in the His bundle and in the right ventricular apex or right ventricular outflow tract for mapping reference and pacing. Access to the left ventricle was obtained using a retroaortic or transseptal approach. Programmed electric stimulation, when performed, delivered up to 3 extra stimuli during 2 paced cycle lengths from 2 right ventricular sites or from the left ventricle. Mapping and ablation were performed using the CARTO system (Biosense Webster, Diamond Bar, California) and an externally irrigated radiofrequency (RF) ablation catheter (NaviStar Thermocool, Biosense Webster).

Endocardial voltage mapping and substrate identification. Detailed endocardial mapping was performed during sinus rhythm or right ventricular apex pacing at 600 ms. To accurately define the VT substrate, multiple sites were explored to obtain a fill threshold of 10 mm within the low-voltage area. The scar mapping was performed as follows.

First, scar voltage limits were set at 1.5 and 0.5 mV to define and measure the scar and dense scar.

Next, electrograms with isolated components and/or late potentials (EIC-LPs) and conduction channels (CCs) were identified and defined during sinus rhythm or right ventricular pacing as previously reported (17,18). An EIC-LP was defined as an electrogram recorded in the scar tissue showing double or multiple components separated by an isoelectric interval ≥50 ms or a very low amplitude signal. A CC was defined as a corridor of continuous electrograms differentiated from the surrounding scar tissue by a higher voltage and connected to normal myocardium by at least 1 site.

Last, pace mapping from EIC-LPs and CCs was performed, attempting to reproduce the documented VT morphology.

After detailed mapping, VT induction was attempted. If VT was induced and mappable, activation mapping was then performed.

Complete endocardial substrate ablation. All patients underwent complete endocardial substrate ablation procedures. This procedure implies that all

TABLE 1 Baseline Characteristics

	All Patients (n = 46)	No Recurrence (n = 29)	Recurrence (n = 17)	p Value
Age (yrs)	68 ± 9	68 ± 10	68 ± 8	0.940
Men	40 (87%)	25 (86%)	15 (88%)	0.844
Hypertension	33 (72%)	22 (76%)	11 (65%)	0.417
Diabetes	21 (46%)	14 (48%)	7 (41%)	0.641
TIA/stroke	10 (22%)	7 (24%)	3 (18%)	0.723
MI location				0.694
Inferior	34 (74%)	22 (76%)	12 (71%)	
Anterior	12 (26%)	7 (24%)	5 (29%)	
Acute reperfusion	11 (24%)	8 (28%)	3 (18%)	0.501
Revascularization	31 (67%)	21 (72%)	10 (59%)	0.343
LVEF by echocardiography (%)	36 ± 10	36 ± 11	37 ± 7	0.625
NYHA functional class				0.619
I/II	42 (91%)	27 (93%)	16 (88%)	
III/IV	4 (9%)	2 (7%)	2 (12%)	
Rhythm				0.820
Sinus rhythm	40 (87%)	25 (86%)	15 (88%)	
Atrial fibrillation	4 (9%)	3 (10.5%)	1 (6%)	
Paced rhythm	2 (4%)	1 (3.5%)	1 (6%)	
Wide QRS complex	17 (37%)	9 (31%)	8 (47%)	0.227
Creatinine (mg/dl)	1.04 ± 0.24	1.07 ± 0.23	0.99 ± 0.26	0.334
Medications				
Beta-blockers	38 (83%)	25 (86%)	13 (76%)	0.443
ACE inhibitors or ARBs	39 (85%)	25 (86%)	14 (82%)	1.000
Amiodarone/sotalol before EPS	12 (26%)	6 (21%)	6 (35%)	0.276
Amiodarone/sotalol after EPS	14 (31%)	8 (28%)	6 (35%)	0.637
Follow-up (months)	32 ± 23	30 ± 26	35 ± 19	0.451
Mortality	4 (9%)	3 (10%)	1 (6%)	1.000
Clinical VT				
Cycle length (ms)	333 (305–394)	359 (301–404)	315 (303–351)	0.131
Nontolerated VT	23 (50%)	14 (50%)	9 (53%)	0.848
Fast VT (<320 ms)	18 (39%)	8 (28%)	10 (59%)	0.045

Values are mean ± SD, n (%), or median (interquartile range).

ACE = angiotensin-converting enzyme; ARB = angiotensin receptor blocker; EPS = electrophysiological study; LVEF = left ventricular ejection fraction; MI = myocardial infarction; NYHA = New York Heart Association; TIA = transient ischemic attack; VT = ventricular tachycardia.

TABLE 2 Electrophysiological Study Data

Electroanatomic Maps	All Patients (n = 46)	No Recurrence (n = 29)	Recurrence (n = 17)	p Value
Number of map points	231 (137–413)	184 (121–351)	330 (186–515)	0.115
Scar area <1.5 mV (cm^2)	64 ± 34	55 ± 28	78 ± 40	0.060
Scar area <0.5 mV (cm^2)	25 ± 20	19 ± 16	34 ± 26	0.032
Total area (cm^2)	170 ± 50	160 ± 42	185 ± 60	0.145
CCs and/or EIC-LPs	40 (89%)	25 (89%)	15 (88%)	1.000
Complete CC and EIC-LP ablation	29 (63%)	20 (69%)	9 (53%)	0.227
Procedure duration (min)	237 ± 100	232 ± 99	246 ± 108	0.743
Fluoroscopy time (min)	34 ± 19	34 ± 19	34 ± 21	0.983
Ablation time (min)	12.3 (7.2–15.9)	11.5 (6.9–15.5)	12.8 (11.7–19)	0.478

Values are median (interquartile range), mean ± SD, or n (%).
CC = conduction channel; EIC-LP = electrogram with isolated components and/or late potentials.

abnormal areas associated with slow conduction, such as EIC-LPs and CCs, are the targets of ablation. EIC-LPs and CCs related to the clinical VT were targeted first and then followed by ablation of all the remaining EIC-LPs and CCs. RF ablation was performed with a 550-kHz RF Stockert-Cordis generator. RF energy was delivered for 60 to 120 s at each ablation site, with a maximum temperature target of 43°C and maximum power of 45 W. Heparin was infused throughout the procedure to maintain an activated clotting time >300 s. Local endpoints were disappearance of EIC-LPs or CCs or absence of local capture at 10 mA × 2 ms. Programmed electric stimulation was repeated only after completing the ablation. Then, any induced VT was targeted if it was mappable or its morphology was similar to the spontaneous or previously induced VT, even if the cycle length was significantly shorter. The morphology of the induced VT was evaluated, the area of the supposedly related scar was revisited, and EIC-LPs and CCs were sought and targeted if identified.

TABLE 3 Magnetic Resonance Imaging Measurements and Signal Intensity Mapping Data

	All Patients (n = 46)	No Recurrence (n = 29)	Recurrence (n = 17)	p Value
MRI measurements				
LVEF (%)	32 ± 10	34 ± 11	30 ± 8	0.235
LV EDV (ml)	240 ± 82	228 ± 88	260 ± 68	0.225
LV ESV (ml)	167 ± 72	156 ± 79	187 ± 57	0.185
LV mass (g)	155 ± 53	146 ± 55	173 ± 44	0.117
FWHM method				
Core infarct mass FWHM (g)	24 ± 13	21 ± 10	31 ± 14	0.014
Core infarct/LV mass (%)	16 ± 8	15 ± 7	19 ± 9	0.206
HT mass FWHM (g)	10 ± 6	10 ± 7	10 ± 4	0.791
HT/LV mass (%)	7 ± 4	7 ± 5	6 ± 3	0.611
Total infarct mass FWHM (g)	34 ± 16	30 ± 15	41 ± 17	0.047
Total infarct/LV mass (%)	23 ± 11	22 ± 10	25 ± 11	0.423
SD method				
Mass >2 SDs (g)	37 ± 15	33 ± 14	44 ± 15	0.026
>2 SDs/LV mass (%)	26 ± 11	25 ± 11	27 ± 11	0.565
Mass >3 SDs (g)	31 ± 14	27 ± 12	37 ± 14	0.029
>3 SDs/LV mass (%)	21 ± 10	21 ± 10	23 ± 11	0.525
HT mass (2–3 SDs) (g)	6 ± 3	6 ± 3	7 ± 3	0.224
HT (2–3 SDs)/LV mass (%)	4 ± 2	4 ± 2	4 ± 2	0.974
SI maps				
Endocardium				
Dense scar (cm^2)	21 ± 15	18 ± 11	28 ± 9	0.019
HT (cm^2)	37 ± 20	30 ± 15	53 ± 21	0.001
Scar (cm^2)	58 ± 27	48 ± 21	81 ± 27	0.001
Epicardium				
Dense scar (cm^2)	15 ± 16	15 ± 18	17 ± 11	0.729
HT (cm^2)	44 ± 23	37 ± 19	59 ± 24	0.008
Scar (cm^2)	59 ± 31	51 ± 29	76 ± 28	0.032

Values are mean ± SD.
EDV = end-diastolic volume; ESV = end-systolic volume; FWHM = full width at half maximum; HT = heterogeneous tissue; LV = left ventricular; LVEF = left ventricular ejection fraction; MRI = magnetic resonance imaging; SI = signal intensity.

FOLLOW-UP. The follow-up protocol included regular clinical and ICD evaluation at 1, 3, and 6 months after the procedure and every 6 months thereafter. The primary endpoint of the study was the recurrence of VT, defined as arrhythmias receiving appropriate ICD therapies or documented sustained monomorphic ventricular tachycardia (SMVT). In all ICDs, the VT zone cutoff was programmed 50 ms longer than the ablated VT cycle length. We analyzed ICD interrogations to differentiate VT and to obtain the number of events, type of therapy required, and VT cycle lengths.

STATISTICAL ANALYSIS. Continuous variables are expressed as mean ± SD or as median and interquartile range (IQR) depending on normality of distribution. Comparisons were performed by Mann-Whitney rank sum or Student *t* tests (paired or unpaired) as appropriate. Categorical variables were compared using Fisher exact tests. The association between endocardial and epicardial contrast-enhanced MRI scar areas was assessed using Pearson correlation. To assess predictors of arrhythmia recurrence, univariate analysis of individual variables was performed using Cox proportional hazards models. The proportional hazards assumption was confirmed analyzing the Schoenfeld residuals. Variables with p values <0.20 were entered in a multivariate analysis (backward selection). Time zero was defined as the time of VT ablation. Optimal cutoff values of scar continuous variables used to predict VT recurrence were determined by time-dependent receiver-operating characteristic curve analysis (19). Scar and HT areas in both endocardium and epicardium were then categorized as large or small using these cutoff values. Kaplan-Meier analysis was used to estimate the event-free rates, and log-rank tests

were used to estimate survival differences. All analyses were performed with IBM SPSS Statistics version 20.0 (SPSS, Chicago, Illinois) and R version 3.1.1 (R Foundation for Statistical Computing, Vienna, Austria). All tests were 2 tailed, and p values <0.05 were considered to indicate statistical significance.

RESULTS

STUDY SAMPLE. Forty-six consecutive patients with SMVT (median cycle length 333 ms; IQR: 305 to 394 ms), chronic myocardial infarction, and previous contrast-enhanced MRI (87% men, mean age 68 ± 9 years, mean LVEF 36 ± 10%) were included in this study. Eighteen patients (39%) had nontolerated fast VT (cycle length ≤320 ms). Baseline characteristics are presented in Table 1.

ELECTROPHYSIOLOGICAL STUDY AND ABLATION PROCEDURE. All patients underwent endocardial electroanatomic mapping. Data from the electrophysiological studies and the ablation procedures are shown in Table 2. Mapping was performed during sinus rhythm in 28 patients (61%), during right ventricular pacing in 17 (37%), and during incessant VT in 1 patient. CCs related to clinical or induced VT and/or EIC-LPs were identified by voltage mapping in 40 subjects (89%). In 17 patients (37%), not all CCs or EIC-LPs could be eliminated. Mean procedure and ablation times were 237 ± 100 min and 12.3 min (IQR: 7.2 to 15.9 min), respectively. No complications related to the ablation procedures occurred.

Inducibility after ablation was suppressed in all but 9 patients (induced VT median cycle length 304 ms; IQR: 240 to 310 ms). In 3 patients, the clinical VT remained inducible, whereas the other 6 patients had nonclinical fast VT.

MRI AND SI MAPPING. Contrast-enhanced MRI and endo-epicardial SI mapping findings are presented in Table 3. Although scar extension was greater in the endocardium than in the epicardium (scar/LV area 42 ± 16% vs. 33 ± 14%, p < 0.001), as was the dense scar/scar area ratio (37 ± 14% vs. 24 ± 15%, p < 0.001), the HT percentage was higher in the epicardium (HT/scar area 63 ± 14% vs. 76 ± 15%, p < 0.001) (Figure 1). A significant positive correlation between the percentage of endocardial and epicardial surface covered by scar was present (r = 0.905, p < 0.001), showing that the larger the endocardial scar, the larger the epicardial scar (Figure 2). Scar areas obtained from SI maps showed a moderate correlation with those obtained from the electroanatomic maps (r = 0.573, p = 0.002).

FOLLOW-UP. During a mean follow-up period of 32 ± 23 months, 29 of 46 patients (63%) were free of

FIGURE 1 Comparison of Percentages of Overall Scar (Scar Area/LV Area), Dense Scar (Dense Scar/Overall Scar Area), and Heterogeneous Tissue (Heterogeneous Tissue/Overall Scar Area) Assessed by Contrast-Enhanced Magnetic Resonance Imaging–Based Signal Intensity Maps in Both Endocardium and Epicardium

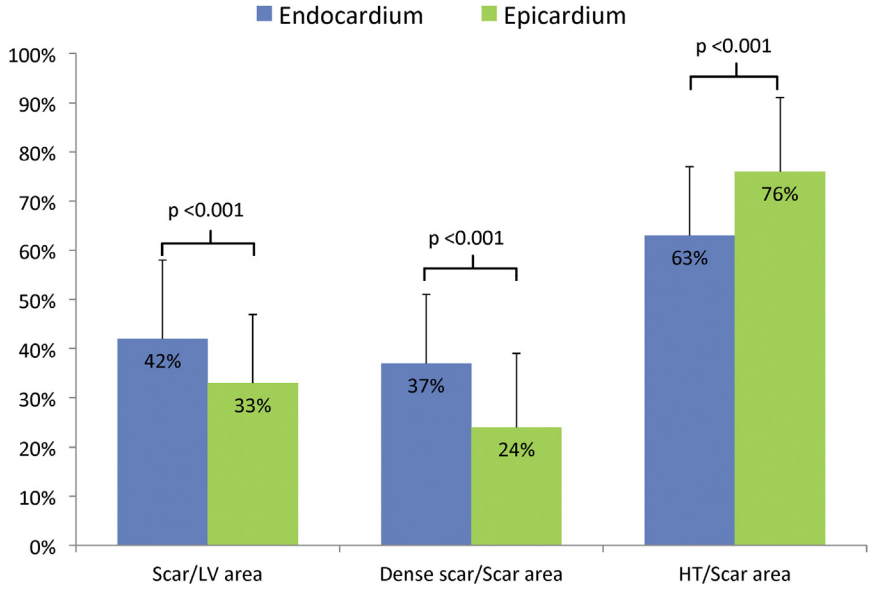

Values are mean percentage ± SD. HT = heterogeneous tissue; LV = left ventricular.

FIGURE 2 Regression Line Showing the Correlation Between the Scar Percentage Identified by Signal Intensity Maps in Both Endocardium and Epicardium

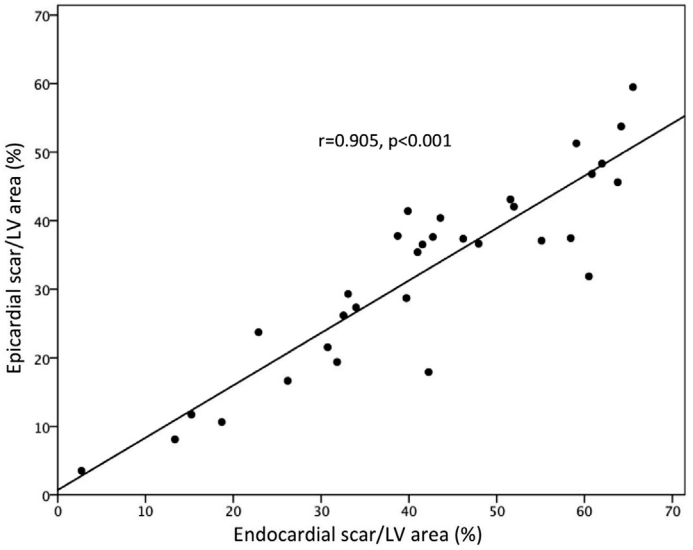

LV = left ventricular.

VT and ICD therapy. Cumulative arrhythmia-free survival was 78% at 1 year, 62% at 3 years, and 40% at 5 years. No patients were lost to follow-up, but 4 died, 1 of heart failure and 3 of noncardiac causes. One patient had VT storm. Ablation was repeated in 9 patients with recurrent episodes and ICD shocks; an epicardial approach was performed in 5 of these patients.

COMPARISON OF PATIENTS WITH AND WITHOUT VT RECURRENCE. No significant differences were found in the demographic characteristics of patients with recurrences at the end of follow-up compared with those without recurrence (Table 1), including similar LVEFs and a comparable use of beta-blockers or antiarrhythmic drugs before and after the ablation.

ELECTROPHYSIOLOGICAL STUDY AND VOLTAGE MAPPING. Induced VT cycle length before ablation was similar in patients with or without recurrences (median 342 ms [IQR: 282 to 400 ms] vs. 313 ms [IQR: 307 to 347 ms], p = 0.527). Larger scars (≤1.5 mV) (78 ± 40 cm^2 vs. 55 ± 28 cm^2, p = 0.06) and specifically larger dense scars (≤0.5 mV) (34 ± 26 cm^2 vs. 19 ± 16 cm^2, p = 0.032) were observed in the electroanatomic maps of patients with VT recurrences (Table 2). No differences between groups were found in the number of CCs, the EIC-LP covered surface, or in the percentage of patients in whom ablation of all these CCs or EIC-LPs could not be achieved. Procedure duration and both fluoroscopy and ablation times were similar in both groups.

MRI and SI mapping data. Despite having similar ejection fractions, patients with VT recurrence had larger infarct masses (31 ± 14 g vs. 21 ± 10 g, p = 0.014) and larger scar and HT areas on SI maps in both endocardium (81 ± 27 cm^2 vs. 48 ± 21 cm^2 [p = 0.007] and 53 ± 21 cm^2 vs. 30 ± 15 cm^2 [p = 0.002], respectively) and epicardium (76 ± 28 cm^2 vs. 51 ± 29 cm^2 [p = 0.032] and 59 ± 24 cm^2 vs. 37 ± 19 cm^2 [p = 0.008]) (Table 3, Figures 3 to 5).

Results from the univariate and multivariate analyses are reported in Table 4. The dense scar area (<0.5 mV) on electroanatomic mapping and both endocardial HT and total endocardial scar on MRI (independently if they were included as continuous or categorical variables), but not infarct mass or other MRI parameters, emerged as predictors of VT recurrence in the univariate analysis. Covariates with p values <0.20 in the univariate analysis were included in the multivariate analysis, as well as LVEF and VT cycle length. MRI endocardial scar extension remained the only independent predictor of VT recurrence (hazard ratio: 1.310 [per 10 cm^2]; 95% confidence interval: 1.05 to 1.63; p = 0.034). Time-dependent receiver-operating characteristic curves for predicting VT recurrence showed (at 54 months): 1) for total endocardia scar, a cutoff point of 65 cm^2 (area under the curve 0.793, sensitivity 81%, specificity 50%); and 2) for endocardial HT, a cutoff point of 45 cm^2 (area under the curve 0.726, sensitivity 72%, specificity 67%). Comparison of the area under the time-dependent receiver-operating characteristic curves confirmed better predictive accuracy of MRI total endocardial scar compared with low-voltage area (<0.5 mV) obtained on electroanatomic mapping (area under the curve at 54 months 0.793 vs. 0.431, p = 0.026).

Patients with large MRI endocardial scars (≥65 cm^2) had a 5-fold increase in the risk for VT recurrence after a complete substrate ablation compared with those with small scars (<65 cm^2) (hazard ratio: 5.32; 95% confidence interval: 1.20 to 25.28; p = 0.035). Kaplan-Meier survival curves for patients with large (vs. small) endocardial HT and total endocardial scar areas are displayed in Figure 6. Patients with smaller MRI endocardial scar area (<65 cm^2) had a higher 5-year probability of VT-free survival compared with those with larger endocardial scar areas (≥65 cm^2) (85% vs. 20%, log-rank p = 0.018). Similarly, cumulative VT-free survival was 14% for patients with endocardial

FIGURE 3 **Comparison of Endocardial and Epicardial Dense Scar, Heterogeneous Tissue, and Total Scar Areas Obtained by Contrast-Enhanced Magnetic Resonance Imaging-Based Signal Intensity Maps in Patients With and Without Arrhythmia Recurrence After Ablation**

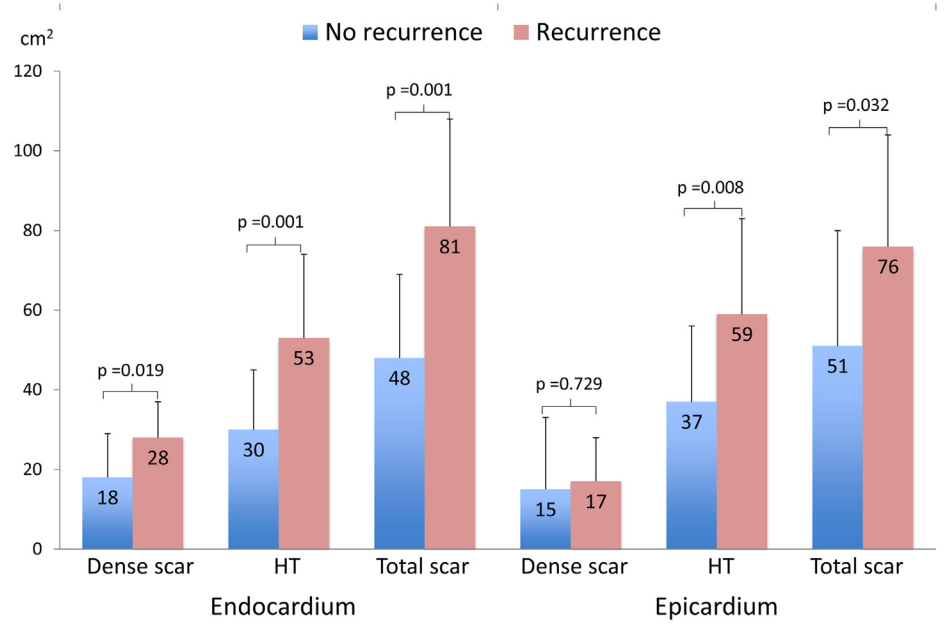

Values are mean ± SD. HT = heterogeneous.

FIGURE 4 **Inferior View of Electroanatomic Map as Well as Endocardial and Epicardial Signal Intensity Maps of a Patient With a Large Myocardial Infarction and Ventricular Tachycardia Recurrence 5 Months After the Ablation Procedure**

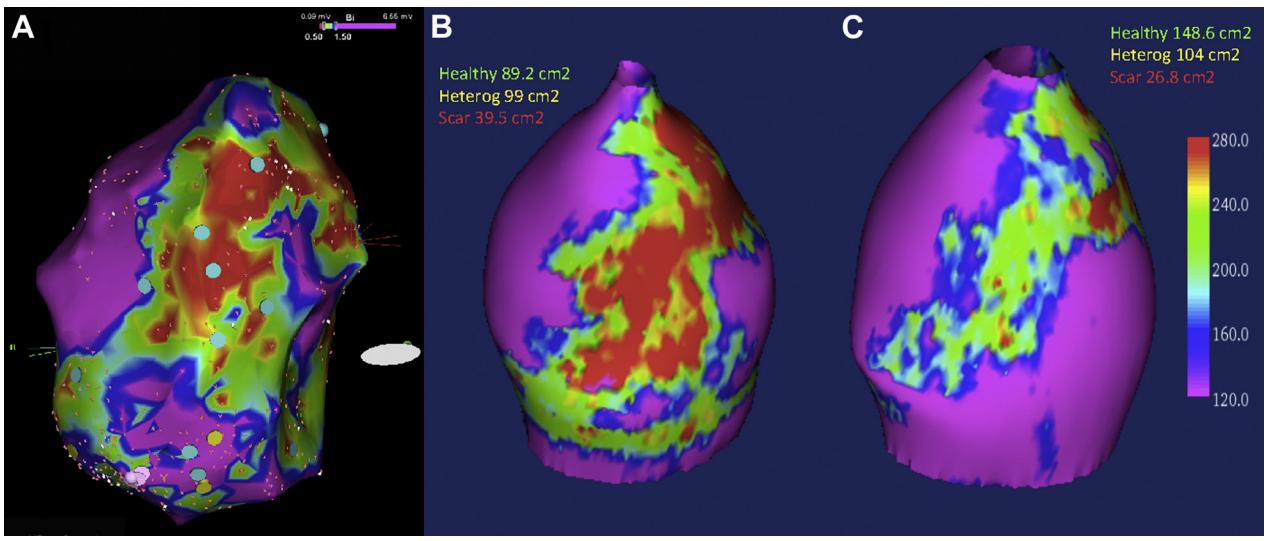

Note the large endocardial scar in the electroanatomic **(A)** and the endocardial signal intensity (SI) map **(B)** as well as the epicardial extension and the amount of heterogeneous tissue (HT) observed in the epicardial SI maps **(C)**. Dense scar, HT, and healthy tissue areas in both endocardial and epicardial SI maps are presented.

JACC: CLINICAL ELECTROPHYSIOLOGY VOL. 1, NO. 5, 2015
OCTOBER 2015:353–65

FIGURE 5 Electroanatomic, Endocardial and Epicardial Signal Intensity Maps of 2 Patients Without Ventricular Tachycardia Recurrence After the Ablation Procedure

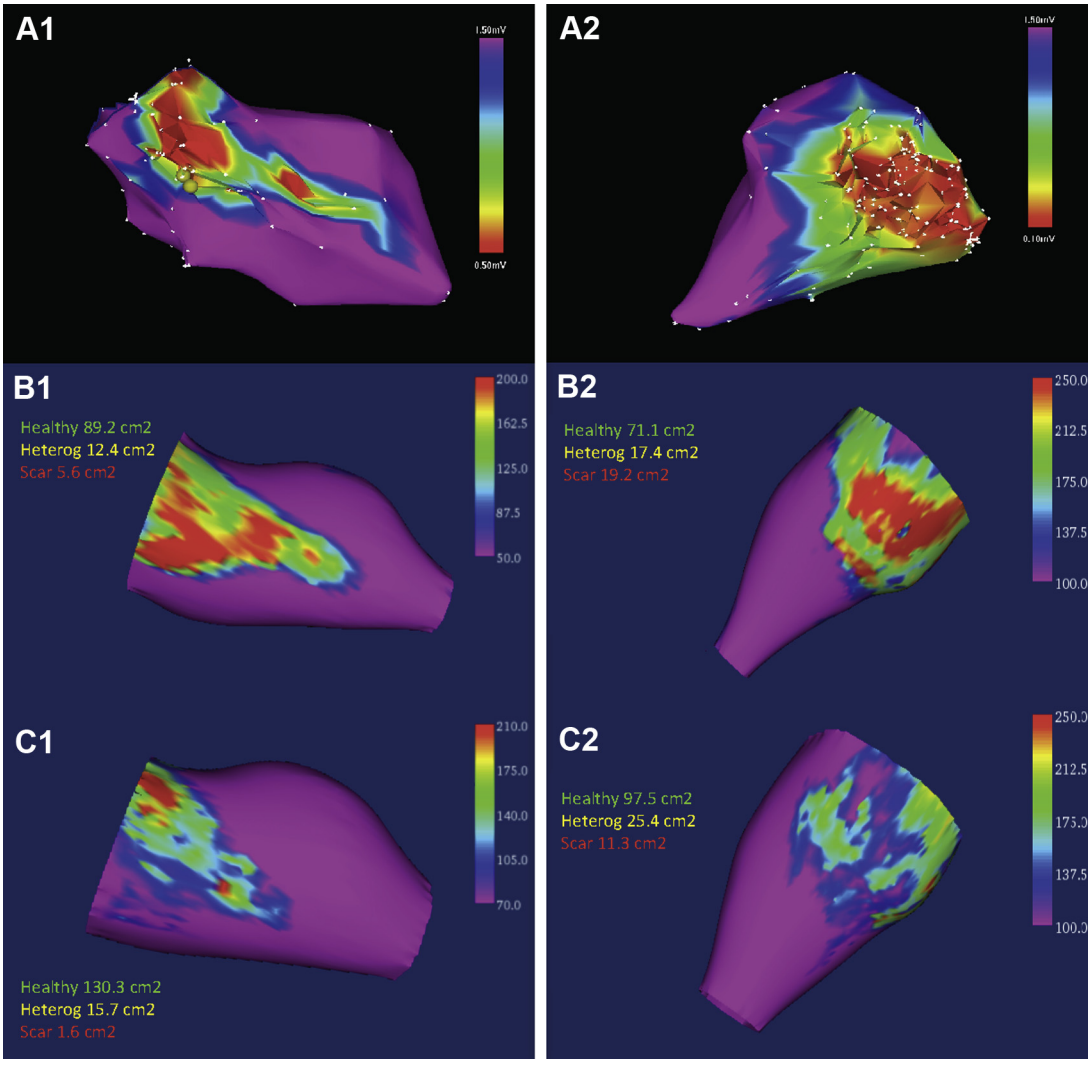

Note the small endocardial scar extension in both the electroanatomic **(A1, A2)** and endocardial signal intensity (SI) maps **(B1, B2)** as well as the small epicardial involvement in the epicardial SI maps **(C1, C2)**. Dense scar, heterogeneous tissue, and healthy tissue areas in all the SI maps are presented.

HT area ≥45 cm^2, compared with 81% in those with endocardial HT area <45 cm^2 (log-rank $p = 0.031$).

RECURRENCE AS EPICARDIAL VT. Repeated ablation procedures were performed in 9 patients. In 5 patients with multiple VT recurrences, epicardial ablation procedures were performed after unsuccessful endocardial approaches. In 4 of these patients, the VT electrocardiographic morphology suggested epicardial origin (Figure 7A). Epicardial VT was related to areas of EIC-LPs that were located in CCs (Figures 7B and 7C). All these patients had extensive epicardial scars in the SI maps (mean HT surface 67 ± 33 cm^2, mean total scar surface 94 ± 35 cm^2) (Figure 7D). Ablation suppressed VT inducibility in 4 of 5 patients. In the 4 remaining patients, new endocardial procedures were performed. In 1 of them, the index procedure had been terminated before all EIC-LPs were eliminated, because of the patient's clinical condition; the clinical VT recurred and was successfully ablated in a second procedure. The other 3 patients presented with new VTs that were successfully ablated from the

endocardium even though during the index procedures, all EIC-LPs had been abolished and only nonclinical VT remained inducible in 2 of them. In all 3 patients, EIC-LPs were present in the second procedure.

DISCUSSION

MAIN FINDINGS. To our knowledge, this is the largest series of patients undergoing post-infarction VT ablation with scar analysis based on contrast-enhanced MRI and the first of its kind describing the usefulness of contrast-enhanced MRI-based SI mapping to predict recurrence after ablation. The main finding of this study is that noninvasive assessment of scar and HT extension predicts VT recurrence.

SUBSTRATE ABLATION STRATEGY. The ablation strategy and the results in terms of VT recurrence obtained in this study are similar to those reported by other groups (4-6,20,21). Only Di Biase et al. (21) reported better outcomes, but this was probably related to the fact that their procedure routinely included epicardial mapping and ablation if needed. The targets of our procedure were mainly low-amplitude late potential electrograms located inside the scar, avoiding larger electrograms located in the border of the scar. This ablation strategy could explain the shorter ablation times (median 12.3 min; IQR: 7.2 to 15.9 min) reported in this study, as abatement of these potential requires less time.

CONTRAST-ENHANCED MRI FOR SCAR AND VT SUBSTRATE ASSESSMENT. This study was on the basis of scar analysis using contrast-enhanced MRI, which several studies have demonstrated is an accurate and reliable method to characterize scar and identify endocardial VT substrate. Infarct surface area, measured by MRI, is a better predictor of inducible VT than LVEF (7). Codreanu et al. (8) and Desjardins et al. (22) compared contrast-enhanced MRI and electroanatomic mapping, showing that critical sites of post-infarction arrhythmias are always confined to areas of high SI. In fact, successful ablation zones appear to be localized in areas of HT, and incomplete ablation in these areas predicted VT recurrence in animal experimental models (23). Perez-David et al. (12) showed a significant correlation in endocardial scar extension detected by SI mapping and electroanatomic mapping as well as in VT-related CC and HT channels (12), findings that were confirmed in later studies (13,14,24).

TABLE 4 Univariate and Multivariate Cox Proportional Analysis for Arrhythmia-Free Survival

	HR	95% CI	p Value
Univariate analysis			
Clinical variables			
Age (per yr)	1.019	0.96–1.08	0.529
LVEF by echocardiography (per 1%)	0.996	0.95–1.04	0.870
Anterior infarction (vs. inferior)	1.627	0.57–4.68	0.366
VT cycle length (per 1 ms)	0.997	0.99–1.00	0.416
Fast VT (<320 ms)	2.203	0.84–5.79	0.109
Use of antiarrhythmic agents post-ablation	2.270	0.83–6.20	0.110
Procedural variables			
Inducibility after ablation	3.452	0.89–13.39	0.073
Incomplete elimination of all CCs and EIC-LPs	1.431	0.55–3.74	0.465
Ablation time (per 1 min)	1.044	0.97–1.123	0.251
Scar area <0.5 mV (per 10 cm^2)	1.350	1.04–1.75	0.017
Scar area <1.5 mV (per 10 cm^2)	1.090	0.97–1.23	0.137
MRI variables			
LVEF by MRI (per 1%)	0.975	0.93–1.03	0.328
FWHM method			
Core infarct mass (per 1 g)	1.030	0.99–1.06	0.155
Core infarct/LV mass (per 1%)	1.014	0.952–1.081	0.661
HT mass (per 1 g)	0.968	0.887–1.056	0.464
HT/LV mass (per 1%)	0.907	0.786–1.047	0.182
Total infarct mass (per 1 g)	1.012	0.982–1.043	0.433
Total infarct/LV mass (per 1%)	0.995	0.949–1.043	0.832
SD method			
Mass >2 SDs (g)	1.026	0.988–1.064	0.181
>2 SDs/LV mass (per 1%)	0.996	0.951–1.043	0.861
Mass >3 SDs (per 1 g)	1.026	0.987–1.066	0.191
>3 SDs/LV mass (per 1%)	0.998	0.951–1.048	0.942
HT mass (2–3 SDs) (per 1 g)	1.042	0.887–1.224	0.617
HT/LV mass (per 1%)	0.896	0.659–1.217	0.482
SI mapping			
Endocardial dense scar (per 10 cm^2)	1.682	0.905–3.096	0.092
Endocardial HT (per 10 cm^2)	1.419	1.07–1.887	0.012
Endocardial scar (per 10 cm^2)	1.310	1.051–1.632	0.010
Epicardial dense scar (per 10 cm^2)	0.970	0.82–1.15	0.849
Epicardial HT (per 10 cm^2)	1.297	0.98–1.68	0.056
Epicardial scar (per 10 cm^2)	1.116	0.93–1.34	0.228
Multivariate analysis			
MRI endocardial scar (per 10 cm^2)	1.310	1.051–1.632	0.034

CI = confidence interval; HR = hazard ratio; SI = signal intensity; other abbreviations as in Tables 1 to 3.

SCAR EXTENSION AND VT RECURRENCE AFTER ABLATION. Although prior reports have described other noninvasive predictors of VT recurrence as nontolerated VT (25) or short cycle length (3), no previous studies have addressed anatomic factors that can be accurately evaluated before the ablation procedure as scar dimensions. Recently, 2 independent studies showed with similar figures that endocardial scar extension measured by voltage mapping during the ablation procedure was larger in patients with VT recurrence after ablation (93 ± 40 cm^2 vs. 69 ± 30 cm^2 in 1 study and

FIGURE 6 Event-Free Survival Curves According to the Endocardial and the Heterogeneous Tissue Area

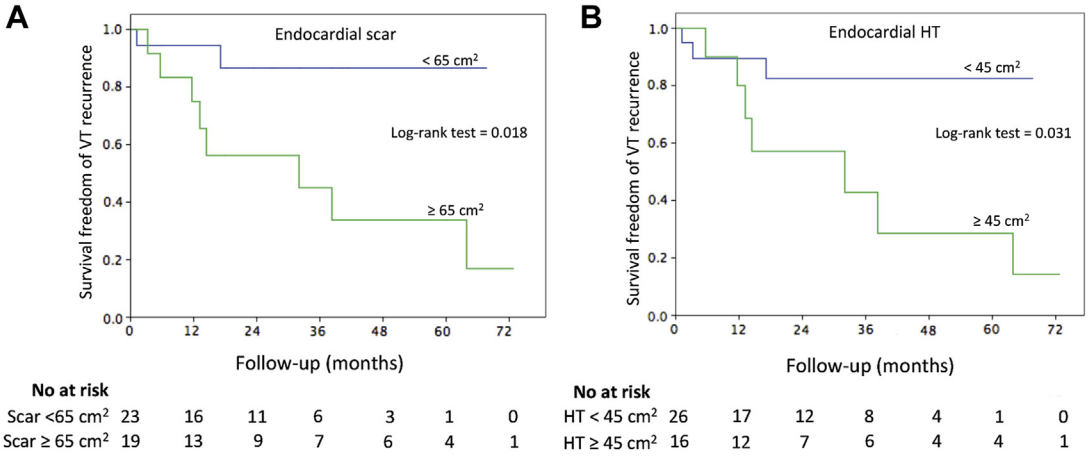

Kaplan-Meier ventricular tachycardia (VT) recurrence-free survival curves according to endocardial scar (cutoff point 65 cm^2) **(A)** and heterogeneous tissue (HT) (cutoff point 45 cm^2) **(B)** as assessed by contrast-enhanced magnetic resonance imaging–based signal intensity mapping.

97 ± 44 cm^2 vs. 60 ± 30 cm^2 in the other); both studies did not find differences in LVEF or infarct location (3,4). Our study supports these previous findings and reinforces the importance of the size of the scar area on VT recurrence: scar area (≤0.5 mV) from electroanatomic mapping and HT and total scar from endocardial and epicardial SI mapping were significantly higher in patients with VT recurrences. Although speculative, it may be plausible that in patients with large HT and scar areas, achieving complete ablation of all areas with EICLPs or local abnormal activity is less likely. This is important, as complete elimination of abnormal activity has been related to a lower risk for VT recurrence (5,6). Also, patients with large HT and scar areas may be more susceptible to develop new arrhythmia circuits in the future. In addition, the larger the MRI endocardial scar, the larger the epicardial scar and, therefore, the probability of epicardial substrate. Almost one-half of the patients in our series who underwent second procedures (4 of 9) had epicardial VT as the cause of the recurrence. These 4 patients had very large epicardial scars on SI maps (**Figure 7**). This finding supports the idea that contrast-enhanced MRI may help identify the epicardial VT substrate, as has been suggested by experimental and clinical studies (26,27). Nonetheless, the small number of patients in which the epicardium was explored precluded any analysis to determine the role of epicardial scar or HT areas in predicting recurrences as epicardial VT.

Interestingly, only scar area obtained from SI mapping (which requires additional MRI processing), but not other measurements of infarct or HT size, such as mass (more easily obtained from MRI analysis), emerged as predictors of VT recurrence. For the same infarct or HT mass, very different scar areas may be found, varying from large scar areas in a very thin wall to small areas in a thick myocardium. These 2 situations are likely to behave in very different ways, as only those with large scars (i.e., larger unexcitable areas) would promote stable circuits leading to VT. In fact, it was recently shown that regional myocardial wall thinning correlates with low-voltage regions and distribution of fragmented electrograms critical for the generation and maintenance of post-infarction VT (28).

CLINICAL IMPLICATIONS. On the basis of these findings, SI mapping obtained by contrast-enhanced MRI could be useful in decisions on VT ablation indications, as in selecting candidates who may benefit from VT ablation (i.e., those with small scars) (1,2). It may also aid in selecting patients in whom not to extend the substrate ablation to the epicardium, thus avoiding unnecessary epicardial explorations. This is very relevant, as in a previous study, more than 65% of pericardial mappings were not followed by ablation (21). Epicardial mapping is thus probably not indicated in patients if little or no epicardial scar is present, even when previous endocardial ablation has

FIGURE 7 **Patient With Multiple Appropriate Discharges After Complete Endocardial Ablation**

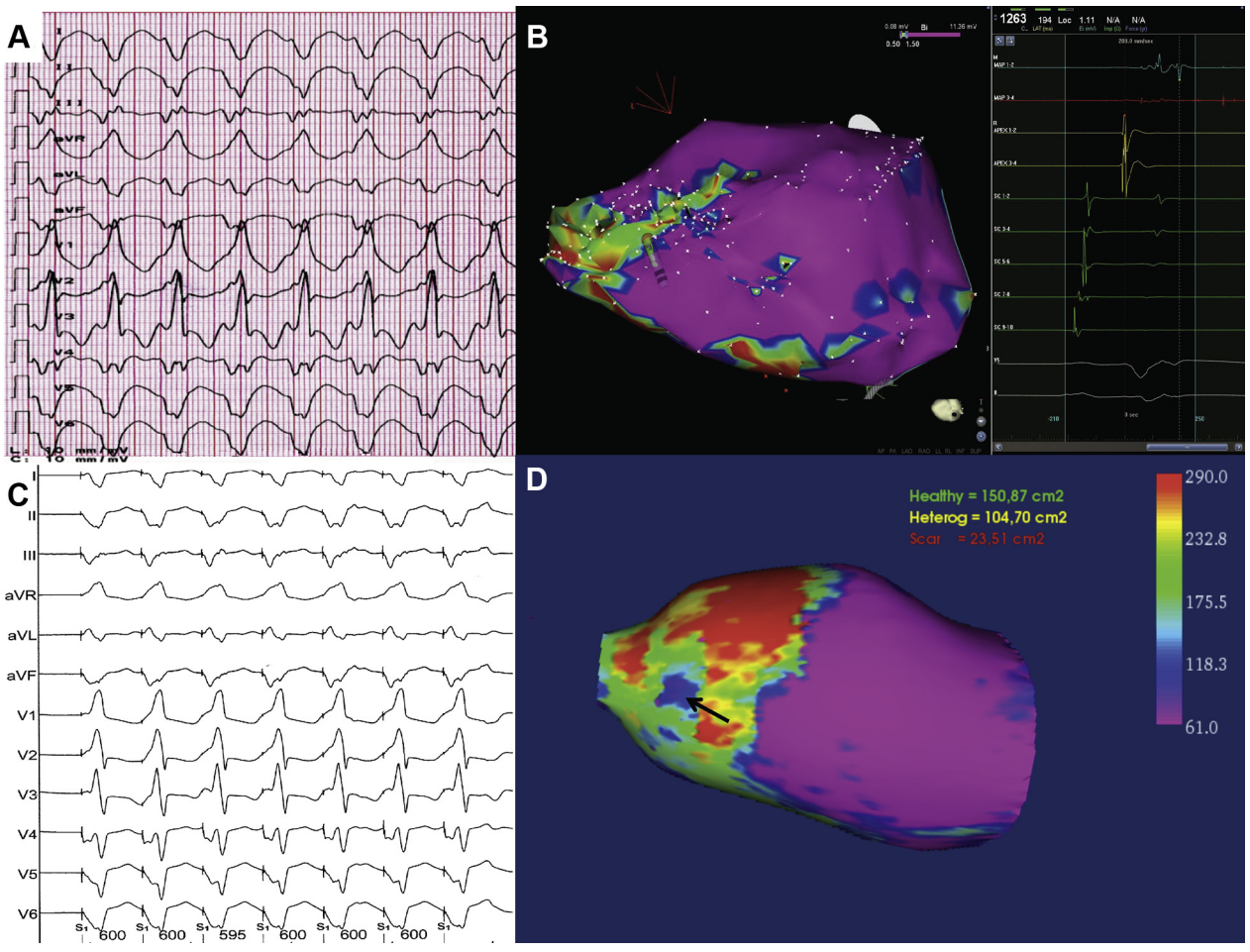

The electrocardiographic ventricular tachycardia (VT) morphology **(A)** suggested an epicardial origin: presence of delta wave in lead V_2 >35 ms, interval to R-wave peak >85 ms. The electroanatomic epicardial voltage map **(B)** illustrates the scar and a channel in segment 1, the catheter tip shows where the electrogram with late potential (right superior corner) was recorded. Pace mapping from this site reproduced the VT morphology **(C)**. This site corresponded to a heterogeneous tissue channel **(black arrow)** in the signal intensity (SI) epicardial map **(D)**. Although the scar seems much larger in the SI than in the electroanatomic map, this mismatch could be due to the fact that epicardial voltage mapping is recording the normal right ventricular wall, which was removed from the SI map. Dense scar, heterogeneous tissue, and healthy tissue areas in the epicardial SI map are presented.

failed. These observations support future clinical studies aimed at defining the role of contrast-enhanced MRI in the context of ablation therapy for post-infarction SMVT.

STUDY LIMITATIONS. Although this is the largest series of patients with contrast-enhanced MRI undergoing post-infarction VT ablation, the main limitation of our study was the small sample size. Most patients requiring VT ablation have ICDs, which is still considered a contraindication to MRI. Nevertheless, MRI-compatible ICDs are being developed, so this problem may be overcome in the coming years. Also, our results are on the basis of patients in whom the epicardium was not explored during the ablation procedure. Thus, we cannot rule out that different predictors would have been found if the epicardium had been explored. Ablation after recurrence was performed in only 9 of 17 patients, so no comprehensive information regarding the location of recurrent VT is available. Finally, only patients with ischemic heart disease were included in this study, so it is unknown if these results could be applied to patients with SMVT due to other cardiomyopathies. Patients with nonischemic cardiomyopathy were excluded, because our algorithm

for obtaining SI maps has not been yet validated in that population.

CONCLUSIONS

Quantification of endocardial and epicardial scar noninvasively by pre-procedural contrast-enhanced MRI-based SI mapping is useful to identify those patients with a higher probability of long-term VT recurrence after complete endocardial substrate ablation. This information could be used for patient selection and to determine the ablation strategy and approach.

ACKNOWLEDGMENT The authors thank Antonio Moratalla for his technical assistance.

REPRINT REQUESTS AND CORRESPONDENCE: Dr. Ángel Arenal, Electrophysiology Unit, Cardiology Department, Hospital General Universitario Gregorio Marañón, Universidad Complutense de Madrid, 46 Dr. Esquerdo Street, 28007 Madrid, Spain. E-mail: arenal@secardiologia.es.

PERSPECTIVES

COMPETENCY IN MEDICAL KNOWLEDGE: The presence of a small endocardial scar, quantified using MRI-based SI maps, is associated with improved long-term procedural outcomes after substrate VT ablation in patients with previous myocardial infarction.

TRANSLATIONAL OUTLOOK: Larger prospective studies are needed to better define the role of pre-procedural MRI scar analysis in acute and long-term ablation outcomes in post-infarction VT.

REFERENCES

1. Reddy VY, Reynolds MR, Neuzil P, et al. Prophylactic catheter ablation for the prevention of defibrillator therapy. N Engl J Med 2007;357:2657–65.

2. Kuck KH, Schaumann A, Eckardt L, et al. Catheter ablation of stable ventricular tachycardia before defibrillator implantation in patients with coronary heart disease (VTACH): a multicentre randomised controlled trial. Lancet 2010;375:31–40.

3. Arenal A, Hernandez J, Calvo D, et al. Safety, long-term results, and predictors of recurrence after complete endocardial ventricular tachycardia substrate ablation in patients with previous myocardial infarction. Am J Cardiol 2013;111:499–505.

4. Yokokawa M, Desjardins B, Crawford T, Good E, Morady F, Bogun F. Reasons for recurrent ventricular tachycardia after catheter ablation of post-infarction ventricular tachycardia. J Am Coll Cardiol 2013;61:66–73.

5. Jais P, Maury P, Khairy P, et al. Elimination of local abnormal ventricular activities: a new end point for substrate modification in patients with scar-related ventricular tachycardia. Circulation 2012;125:2184–96.

6. Vergara P, Trevisi N, Ricco A, et al. Late potentials abolition as an additional technique for reduction of arrhythmia recurrence in scar related ventricular tachycardia ablation. J Cardiovasc Electrophysiol 2012;23:621–7.

7. Bello D, Fieno DS, Kim RJ, et al. Infarct morphology identifies patients with substrate for sustained ventricular tachycardia. J Am Coll Cardiol 2005;45:1104–8.

8. Codreanu A, Odille F, Aliot E, et al. Electroanatomic characterization of post-infarct scars comparison with 3-dimensional myocardial scar reconstruction based on magnetic resonance imaging. J Am Coll Cardiol 2008;52:839–42.

9. Klem I, Weinsaft JW, Bahnson TD, et al. Assessment of myocardial scarring improves risk stratification in patients evaluated for cardiac defibrillator implantation. J Am Coll Cardiol 2012;60:408–20.

10. Schmidt A, Azevedo CF, Cheng A, et al. Infarct tissue heterogeneity by magnetic resonance imaging identifies enhanced cardiac arrhythmia susceptibility in patients with left ventricular dysfunction. Circulation 2007;115:2006–14.

11. Roes SD, Borleffs CJ, van der Geest RJ, et al. Infarct tissue heterogeneity assessed with contrast-enhanced MRI predicts spontaneous ventricular arrhythmia in patients with ischemic cardiomyopathy and implantable cardioverter-defibrillator. Circ Cardiovasc Imaging 2009;2:183–90.

12. Perez-David E, Arenal A, Rubio-Guivernau JL, et al. Noninvasive identification of ventricular tachycardia-related conducting channels using contrast-enhanced magnetic resonance imaging in patients with chronic myocardial infarction: comparison of signal intensity scar mapping and endocardial voltage mapping. J Am Coll Cardiol 2011;57:184–94.

13. Andreu D, Berruezo A, Ortiz-Perez JT, et al. Integration of 3D electroanatomic maps and magnetic resonance scar characterization into the navigation system to guide ventricular tachycardia ablation. Circ Arrhythm Electrophysiol 2011;4:674–83.

14. Fernandez-Armenta J, Berruezo A, Andreu D, et al. Three-dimensional architecture of scar and conducting channels based on high resolution ce-CMR: insights for ventricular tachycardia ablation. Circ Arrhythm Electrophysiol 2013;6:528–37.

15. Amado LC, Gerber BL, Gupta SN, et al. Accurate and objective infarct sizing by contrast-enhanced magnetic resonance imaging in a canine myocardial infarction model. J Am Coll Cardiol 2004;44:2383–9.

16. Yan AT, Shayne AJ, Brown KA, et al. Characterization of the peri-infarct zone by contrast-enhanced cardiac magnetic resonance imaging is a powerful predictor of post-myocardial infarction mortality. Circulation 2006;114:32–9.

17. Arenal A, Glez-Torrecilla E, Ortiz M, et al. Ablation of electrograms with an isolated, delayed component as treatment of unmappable monomorphic ventricular tachycardias in patients with structural heart disease. J Am Coll Cardiol 2003;41:81–92.

18. Arenal A, del Castillo S, Gonzalez-Torrecilla E, et al. Tachycardia-related channel in the scar tissue in patients with sustained monomorphic ventricular tachycardias: influence of the voltage scar definition. Circulation 2004;110:2568–74.

19. Hung H, Chiang C-T. Estimation methods for time-dependent AUC models with survival data. Can J Stat 2010;38:8–26.

20. Carbucicchio C, Ahmad Raja N, Di Biase L, et al. High-density substrate-guided ventricular tachycardia ablation: role of activation mapping in an attempt to improve procedural effectiveness. Heart Rhythm 2013;10:1850–8.

21. Di Biase L, Santangeli P, Burkhardt DJ, et al. Endo-epicardial homogenization of the scar versus limited substrate ablation for the treatment of electrical storms in patients with ischemic cardiomyopathy. J Am Coll Cardiol 2012;60:132–41.

22. Desjardins B, Crawford T, Good E, et al. Infarct architecture and characteristics on delayed enhanced magnetic resonance imaging and

electroanatomic mapping in patients with post-infarction ventricular arrhythmia. Heart Rhythm 2009;6:644–51.

23. Estner HL, Zviman MM, Herzka D, et al. The critical isthmus sites of ischemic ventricular tachycardia are in zones of tissue heterogeneity, visualized by magnetic resonance imaging. Heart Rhythm 2011;8:1942–9.

24. Piers SR, Tao Q, de Riva Silva M, et al. CMR-based identification of critical isthmus sites of ischemic and nonischemic ventricular tachycardia. J Am Coll Cardiol Img 2014;7:774–84.

25. Della Bella P, Baratto F, Tsiachris D, et al. Management of ventricular tachycardia in the setting of a dedicated unit for the treatment of complex ventricular arrhythmias: long-term outcome after ablation. Circulation 2013;127:1359–68.

26. Arenal A, Perez-David E, Avila P, et al. Noninvasive identification of epicardial ventricular tachycardia substrate by magnetic resonance-based signal intensity mapping. Heart Rhythm 2014;11:1456–64.

27. Andreu D, Ortiz-Perez JT, Boussy T, et al. Usefulness of contrast-enhanced cardiac magnetic resonance in identifying the ventricular arrhythmia substrate and the approach needed for ablation. Eur Heart J 2014;35:1316–26.

28. Komatsu Y, Cochet H, Jadidi A, et al. Regional myocardial wall thinning at multidetector computed tomography correlates to arrhythmogenic substrate in postinfarction ventricular tachycardia: assessment of structural and electrical substrate. Circ Arrhythm Electrophysiol 2013;6:342–50.

KEY WORDS **catheter ablation, magnetic resonance imaging, myocardial infarction scar, recurrence, ventricular tachycardia**